TECHNISCHE MECHANIK, Band 25, Heft 3-4, (2005), 162– 173
Manuskripteingang: 15.04.2005

Hyperelastic Description of Polymer Soft Foams at Finite Deformations

M. Schrodt , G. Benderoth, A. Kühhorn, G. Silber

Soft foams are gaining importancy as materials for mattress systems and seat cushions in such areas as aircraft and automotive industries and in the field of medical care. This study will demonstrate that a strain energy function of finite hyperelasticity for compressible media proposed by Hill (1978), Storakers (1986) and Ogden (1972) is applicable to describe the elastic properties of open cell soft foams. This strain energy function is implemented in the FE-tool ABAQUS and proposed for high compressible soft foams. To determine this constitutive equation, experimental data from a uniaxial compression test are used. As the parameters in the constitutive equation are linked in a non-linear way, non-linear optimisation routines are adopted. Moreover due to the inhomogeneities of the deformation field of the uniaxial compression test, the quality function of the optimisation routine has to be determined by an FE-tool. The appropriateness of the strain energy function is tested by a complex loading test. By using the optimised parameters the FE-simulation of this test is in good accordance with the experimental data.

1 Introduction

The optimisation of mattress systems and seat cushions is becoming more and more important in such areas as aircraft, automotive industries and medical care. Due to the great variety of designable mechanical properties and the low cost of production, soft foams are more widely used for such systems. In spite of the more frequent usage of soft foams, there are very few publications concerning their mechanical behaviour. According to DIN 7726, soft foams are considered as a two-phase system where a gas (e.g. air) is dispersed in a continuous solid matrix (cell structure) (Lenz, 1999).

For the mechanical description of hard foams, there are three articles from Renz (1977), Renz (1978) and Czysz (1986) where the last author describes Polyurethan soft foam by Hooke elasticity. Presently, non-linear models for soft foams are in general based on a hyperelastic approach for compressible media with a particular strain energy function. Most of these approaches are based on a strain energy function for incompressible media proposed by Ogden (1972) which is extended to the compressible case by the third invariant of the deformation gradient. In most of these models the deformation gradient as well as the strain energy is splitted in a volumetric and a isochoric part (Simo and Taylor, 1991), which leads in the case of large deformations, to nonphysical effects according to a study by Eipper (1998). Additionally, there are ambitious continuum models based on a detailed description of the inner structure of the foam. Ehlers and Markert (2001) apply a theory of mixtures of multiphase materials based on a continuum mechanical theory of porous media to soft foams, whereby the solid-fluid-problem can be solved. Wang and Cuitino (2000) introduce a hyperelastic continuum model based on the description of the tension/compression and bending loading of a single cell and on an irregular shaped open cell structure. An analysis based on an FE method for open cell Polyurethan soft foams was carried out by Mills and Gilchrist (2000) using the a strain energy function for high compressive soft foams (so-called Hyperfoam) has been implemented in the FE-program ABAQUS (Hibbitt et al., 2000a), (Hibbitt et al., 2000b). But this study comprises only parameter studies compared with experimental data and no stringent parameter identification was done. Additionally, for the volume strain the important parameter β was ruled out so that the appropriateness of the model for the examined material becomes questionable.

The objective of this study is to apply an implemented strain energy function “Hyperfoam” in ABAQUS to describe the mechanical properties of soft foams. This will be done by adequate experiments and a stringent parameter identification. The identification is carried out by non-linear optimisation routines where the simulation of an uniaxial compression test is used to solve the quality function. The parameter vector derived in such a way is used for the simulation of an indenter test. The comparison of this simulation with the experimental data shows

the appropriateness of this strain energy function. The investigation is restricted to the elastic properties of the foams only, thus these properties are separated from the inelastic ones by suitable experiments with holding times. Furthermore, the Mullins (1969) effect is eliminated by a cyclic preprocess of the test specimen at the beginning of each experiment.

2 Experiments

Figure 1: Buckling of a cubic test specimen at a uniaxial compression test

Test specimens of polyurethane soft foam called SAF 6060 were provided by a Swiss soft foam producer (Foam Partner Fritz Nauer AG). The test specimens are cubes with a quadratic cross section of 200 by 200 mm and a height of 50 mm randomly taken out of a complete mattress. The used test specimens differ in geometry from a standard one (100 mm by 100 mm by 100 mm) because cubic test specimens show buckling at the uniaxial compression test (see Figure1). The tested foam shows an open cell structure and has a density of 60 kg/m^3 and a compression load deflection of 6 kPa. All forces shown in the figures are pressure loads.

Laboratory tests show a significant dependency of the mechanical behaviour of the foams on temperature and humidity (Figure 2), thus all tests were carried out at constant climatic conditions (20 $^\circ$C temperature and 50% humidity).

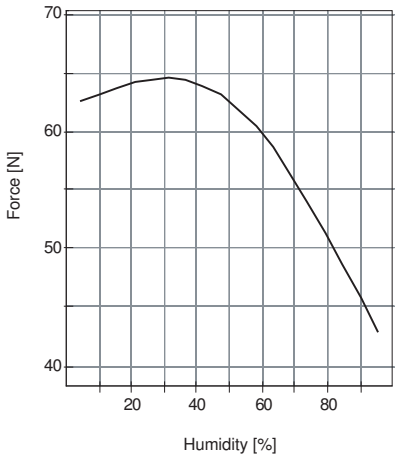

Figure 2: Tests of the climatic dependency of the material properties for SAF 6060.

Beside the material's dependency on temperature and humidity, it shows a combination of elastic and inelastic behaviour. To separate these properties, a testing procedure proposed by James and Green (1975) and Van den Bogert

and de Borst (1994), successfully applied by Hartmann et al. (2003) and Lion (1996) for rubber like materials, was also used here.

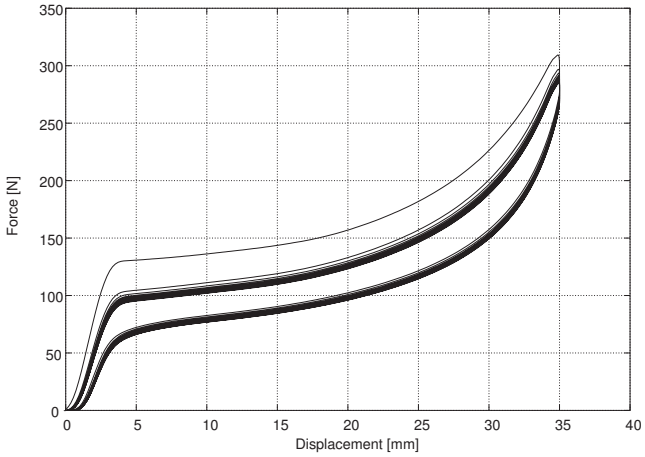

Figure 3: MULLINS effect of a test specimen

Cyclic preprocess: To eliminate the Mullins (1969) effect (Chagnon et al., 2002) (see Figure 3) a procedure consisting of a strain-controlled cyclic deformation of 70% with a strain rate of 0.2 s^{-1} followed by a load discharge was applied. This cycle was redone 16 times (see Figure 4).

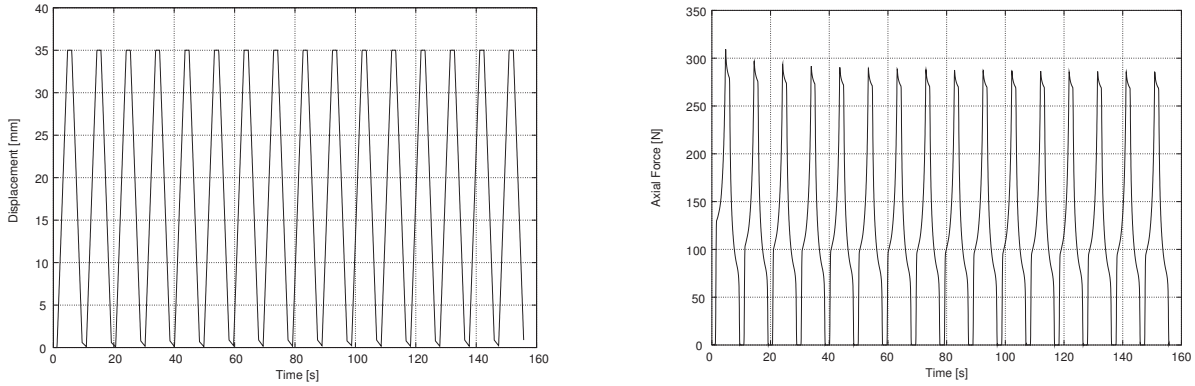

Figure 4: Cyclic preprocess with constant displacement amplitude and force relaxation

Experiments with holding times: After a recovery phase of 16 hours a step-by-step deformation with a constant strain rate of 0.2 s^{-1} was applied to each test specimen. After each deformation step a holding time of 180 min was applied to the specimen (see Figure 5). During this holding time the material responded with a relaxation. This procedure ought to ensure that the responding force has reached an equilibrium state so that the termination points of relaxation represent the equilibrium state of the material (Ehlers and Markert, 2001). The holding time ensures that the time derivative of the stress was close to zero. Despite the fact that the stress rate was almost zero, the relaxation process was still ongoing (see e.g. Figure 7). For the sake of performing a managable experiment, a termination of three hours for each step was taken. All the termination points of the holding time generated an equilibrium stress-strain curve. The difference between the termination of the deformation steps and its corresponding equilibrium point is called overstress. After performing the final deformation step an unloading phase was applied. This process was exactly the reverse of the loading process (Figure 5). For getting an appropriate data set for the parameter optimisation, different intervals for the holding points over the deformation course have been chosen. Figure 3 shows that the slope of the deformation course is up to a value of displacement of 4 mm much steeper than in the following sections. Thus holding points at 1, 2 and 4 mm were chosen. For larger displacement values a constant interval of 4 mm was taken.

Two different types of tests were carried out. A uniaxial compression test and a test with an indenter (a cylinder with a spherical calotte of 50 mm diameter at its end (Figure 6)).

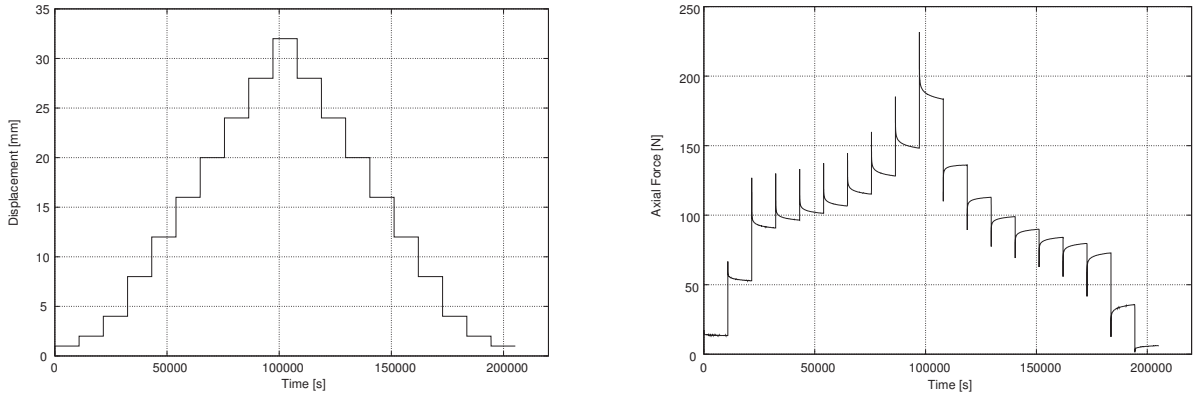

Figure 5: Experiment with holding times, loading and unloading path for holding time experiments and force response with relaxation

Figure 6: Test Configurations

To establish a homogeneous deformation field, the shear stresses between the two plates on top and bottom side and the test specimen at the uniaxial compression test has to be eliminated. This turned out to be rather difficult to achieve. For having defined boundary conditions, the test specimen were fixed at the two plates (Figure 6). The boundary condition causes a reversible bulge at the edges of the test specimen while being tested.

To generate a spatially defined deformation field, an indenter type test was carried out. In this test a spherical calotte (diameter of 50 mm) is pushed down into the test specimen, where the penetration depth and the associated normal force was measured during the penetration process.

3 Constitutive Equation

3.1 General Constitutive Equation for Hyperelastic Materials

According to the results of the empirical analysis, the considered soft foams show a compressible viscoelastic material behaviour. To describe this phenomenon, a viscoelastic constitutive equation is usually adopted. In general, viscoelastic models decompose the total stress tensor $\boldsymbol{S}$ into an (elastic) equilibrium stress part $\boldsymbol{S}_G$ and an overstress part $\boldsymbol{S}_{OV}$ representing the memory property of the material. Thus the stress tensor can be written as $\boldsymbol{S} = \boldsymbol{S}_G + \boldsymbol{S}_{OV}$ (see Hartmann et al. (2001)). This study will exclusively deal with the elastic properties of soft foams according to the empirically attained stress-strain curves of the termination points after a distinct holding time (see the last section). For such a description, constitutive equations for hyperelasticity are permissible (Hartmann et al., 2003). For the sake of simplicity, the index G in the above formula will be left out for further

discussion.

Hyperelastic materials represent a subset of (CAUCHY-) elastic materials characterised by an elastic potential (strain energy function). The stress tensor can be generated by the derivation of the strain energy function with regard to the strain tensor. The basis therefore is the equation of mechanical energy

$$\dot{w} = J\boldsymbol{S} \cdot\cdot \boldsymbol{D} \qquad \text{with} \qquad J = \det \boldsymbol{F} \tag{1}$$

where w is the strain energy function, $\boldsymbol{F}$ the deformation gradient, $\boldsymbol{S}$ the CAUCHY stress tensor and $\boldsymbol{D}$ the strain rate tensor

$$\boldsymbol{D} = \frac{1}{2}\boldsymbol{F}^{-T} \cdot \dot{\boldsymbol{C}} \cdot \boldsymbol{F}^{-1} \tag{2}$$

with the right CAUCHY-GREEN tensor $\boldsymbol{C}$ (a dot above the symbol means the material time derivative). Due to the principle of objectivity, w has to be a scalar-valued non-negative tensor function of the right stretch tensor $\boldsymbol{U}$ or the right CAUCHY-GREEN tensor

$$w = w\left(\boldsymbol{U}\right) = w\left(\boldsymbol{C}\right) = \begin{cases} > 0 & \text{for} \quad \boldsymbol{C} \neq \boldsymbol{I} \\ = 0 & \text{for} \quad \boldsymbol{C} = \boldsymbol{I} \end{cases} \tag{3}$$

According to (3) in the undeformed state (reference configuration ($\boldsymbol{C} = \boldsymbol{I}$) the strain energy w is always zero and for the deformed state (current configuration ($\boldsymbol{C} \neq \boldsymbol{I}$) the strain energy always has to be non-negative ($w > 0$). Inserting (3) into (1) by regarding (2) results in the most general structure of the constitutive equation for non-linear, hyperelastic, anisotropic material behaviour (Green and Adkins, 1970):

$$\boldsymbol{S} = 2\, J^{-1}\boldsymbol{F} \cdot \frac{\partial w\left(\boldsymbol{C}\right)}{\partial \boldsymbol{C}} \cdot \boldsymbol{F}^{T} \tag{4}$$

3.2 Strain Energy Function for Highly Compressible Polymers

For describing the mechanical behaviour of highly compressible polymers, the following strain energy function has been proposed by Hill (1978) and Storakers (1986)

$$w = \sum_{k=1}^{N} 2\frac{\mu_k}{\alpha_k^2}\left[\lambda_1^{\alpha_k} + \lambda_2^{\alpha_k} + \lambda_3^{\alpha_k} - 3 + f(J)\right] \tag{5}$$

where μ_κ and α_κ are material parameters and $f(J)$ a volumetric function, which has to fulfil the restriction $f(1) = 0$. Using (5) one gets for the spectral representation of (4)

$$\boldsymbol{S} = 2J^{-1}\sum_{i=1}^{3}\sum_{k=1}^{N}\left\{\frac{\mu_k}{\alpha_k}\left[\lambda_i^{\alpha_k} + \frac{1}{\alpha_k}J\frac{\partial f\left(J\right)}{\partial J}\right]\boldsymbol{n}_i\boldsymbol{n}_i\right\} \tag{6}$$

with the eigenvalues λ_i of the right stretch tensor $\boldsymbol{U}$ and the eigenvectors $\boldsymbol{n}_i$ of the left stretch tensor $\boldsymbol{V}$. A possible form of the volumetric function $f(J)$ is given by Storakers (1986)

$$f(J) = \frac{1}{\beta_k}\left(J^{-\alpha_k\beta_k} - 1\right) \tag{7}$$

where β_k are additional material parameters. Thus one gets $3N$ material coefficients α_k, β_k and μ_k ($k = 1, 2, ..., N$) which in general have to be determined by appropriate tests. Additionally the initial shear modulus and compression modulus are defined by (Hibbitt et al., 2000a)

$$\mu_0 := \sum_{i=1}^{N} \mu_i \qquad \text{and} \qquad \kappa_0 := \sum_{i=1}^{N} 2\left(\frac{1}{3} + \beta_i\right)\mu_i \tag{8}$$

There is also a relation given between the Poisson's ratios ν_i and the parameters β_i

$$\nu_i = \frac{\beta_i}{1 + 2\beta_i} \qquad \text{respectively} \qquad \beta_i = \frac{\nu_i}{1 - 2\nu_i} \quad i = 1, 2, ..., N \tag{9}$$

For the particular case $\beta_i =: \beta = const$, ν is the classical Poisson's ratio. For the parameters in (6) and (7) certain restrictions have to be fulfilled (extensively discussed in Reese (1994)). According to Hill (1978) and Storakers (1986) the following unequalities shall always be valid (the second unequality holds for the particular case $\beta_i =: \beta = const$ only)

$$\mu_k \alpha_k > 0 \quad (k = 1, 2, ..., N)\text{(no sum) and} \quad \beta > -\frac{1}{3} \tag{10}$$

3.3 Force-stretch-relation for the Uniaxial Compression Test

Considering a homogeneous deformation state the deformation gradient is

$$\boldsymbol{F}(t) = \lambda_1(t)\,\boldsymbol{e}_1\boldsymbol{e}_1 + \lambda_2(t)\,\boldsymbol{e}_2\boldsymbol{e}_2 + \lambda_3(t)\,\boldsymbol{e}_3\boldsymbol{e}_3 \tag{11}$$

with the stretches

$$\lambda_1 = \lambda_2 = \frac{a(t)}{a_0} \quad , \quad \lambda_3 = \frac{h(t)}{h_0} \quad , \quad J = \lambda_1^2\lambda_3 = \left[\frac{a(t)}{a_0}\right]^2 \frac{h(t)}{h_0} \tag{12}$$

where a_0 and $a(t)$ are the angle lengths and h_0 and $h(t)$ are the heights of a test specimen in the undeformed and deformed state.

If the specimen is loaded only in the 3-direction according to the homogeneous deformation there is no stress in 1- or 2-direction. Thus according to (6) by obeying $(7)_2$ and (12) the stress state has the following form:

$$\begin{aligned} \sigma_{33}(\lambda_1, \lambda_3) &= 2\left(\lambda_1^2\lambda_3\right)^{-1} \sum_{k=1}^{N} \frac{\mu_k}{\alpha_k}\left[\lambda_3^{\alpha_k} - \left(\lambda_1^2\lambda_3\right)^{-\alpha_k\beta_k}\right] \\ 0 &= \sum_{k=1}^{N} \frac{\mu_k}{\alpha_k}\left[\lambda_1^{\alpha_k} - \left(\lambda_1^2\lambda_3\right)^{-\alpha_k\beta_k}\right] \end{aligned} \tag{13}$$

If a specimen is loaded by a single load K in the 3-direction, the stress in the 3-direction by regarding the equilibrium condition will be $\sigma_{33} = -K/(ab) \equiv -K/a^2$. Thus the final relation for the uniaxial loading is

$$K(\lambda_1, \lambda_3) = -2a^2\left(\lambda_1^2\lambda_3\right)^{-1} \sum_{k=1}^{N} \frac{\mu_k}{\alpha_k}\left[\lambda_3^{\alpha_k} - \left(\lambda_1^2\lambda_3\right)^{-\alpha_k\beta_k}\right] \tag{14}$$

and the following implicit relation holds for the stretches in 1- and 2-direction λ_1 and λ_2 due to $(13)_2$

$$f(\lambda_1, \lambda_3) = \sum_{k=1}^{N} \frac{\mu_k}{\alpha_k} \left[\lambda_1^{\alpha_k} - \left(\lambda_1^2 \lambda_3 \right)^{-\alpha_k \beta_k} \right] = 0 \tag{15}$$

For the particular case $N = 1$ and using $\alpha_1 := \alpha$, $\beta_1 := \beta$, $\mu_1 := \mu$ one can derive an explicit relation between λ_1 and λ_3

$$\lambda_1 = f(\lambda_3) = \lambda_3^{-\frac{\beta}{1+2\beta}} \quad \text{and finally} \quad \lambda_1^2 \lambda_3 = \lambda_3^{\frac{1}{1+2\beta}} \tag{16}$$

Equation (16) allows a separation of the material parameter β from the rest and can be used for a separate analysis of β (see Storakers (1986)). By using (16) λ_1 can be eliminated from (9) in the case *N*=1. Thus the final form of the force-stretch-relation (8) reads (*N* = 1)

$$K(h) = 2\frac{\mu}{\alpha} a_0^2 \left[\left(\frac{h}{h_0} \right)^{-\alpha \frac{1+3\beta}{1+2\beta}} - 1 \right] \left(\frac{h}{h_0} \right)^{\alpha - 1} \equiv 2\frac{\mu}{\alpha} a_0^2 \left(\lambda_3^{-\alpha \frac{1+3\beta}{1+2\beta}} - 1 \right) \lambda_3^{\alpha - 1} \tag{17}$$

On the basis of the expression (17) the importance of restriction $(10)_2$ is evident, because for $\beta = -1/3$ the value of K would be always zero for arbitrary stretches λ_3.

4 Parameter Optimisation

The basic aim is to describe the elastic properties of the material by the constitutive equations (6) and accordingly (14), (15) or (17), so that these functions reproduce the empirical data in an appropriate way. This is obtained by using a quality function Φ of the following form

$$\Phi := \frac{1}{n} \sqrt{\sum_{i=1}^{n} \left[f(h; \alpha_1, ..., \alpha_N) - f_i(h_i) \right]^2} \stackrel{!}{=} \min \tag{18}$$

where $f(h; \alpha_1, \ldots, \alpha_N)$ is the model with h the independent variable, the $\alpha_1, \ldots, \alpha_N$ are arbitrary model parameters and f_i and h_i are the measured values. In this particular case, the model is the constitutive equation (17) with the displacement coordinate h and the axial force f as independent and dependent variable, μ_j, α_j and β_j are the model parameters. The values for the f_i and h_i were taken from the measured data of the uniaxial compression test described in Section 2.

Optimisation routines: As most of the parameters within the constitutive equations appear in a non-linear way, for minimising the quality function (18) a non-linear optimisation routine has to be used for this purpose. The authors chose a stochastic and a deterministic routine. The stochastic routine is a modified MONTE CARLO routine called SIMULATED ANNEALING (Otten and van Ginneken, 1989). This routine was used to evaluate the material parameters for the constitutive equation (17) for the uniaxial compression test.

A stochastic routine rather ensures to find the global minimum compared to deterministic routine at the expanse of extensive usage of function evaluation. Thus for using the FE- program for the function evaluation, the deterministic SIMPLEX STRATEGY (Nelder and Mead, 1969) was taken. Because of the particular boundary conditions of the uniaxial compression test, the FE-program was used for determining the parameters of (6). As starting values for this parameter determination the results of the fit for equation (17) were taken.

Both routines were coded by the authors according to algorithms given by Schwefel (1995).

5 Finite Element Simulation

To verify the appropriateness of the constitutive model describing the mechanical behaviour of soft foams, the compression and the indenter type test as well have to be simulated by an FE-simulation.

The indenter type and uniaxial compression test were solved with 8-node linear brick elements. The bottom surface of the foam was constrained in x-, y- and z-directions, whereas the top surface was only restricted in x- and z-directions. A constant displacement was imposed to represent the testing scenario. In the case of the indenter test, the indenter itself was modelled as a rigid body. A constant friction coefficient of 0.75 was used between the indenter surface and the foam surface with the same constraints for the bottom surface as in the uniaxial load test. For the sake of comparison between the experimental data and the results of the FE-simulation in the case of the uniaxial loading, the sum of the resulting forces in loading direction at surface nodes was taken. For the case of the indenter test, the resulting force of the rigid body in loading direction was used.

6 Results

Figure 7 shows the experimental results of the uniaxial compression test. It can be seen, that even holding times of 180 min are too short, since the overstresses are not completely relaxed. Hence, there is a very small hysteresis defined by the termination points of relaxation (the equilibrium points are only reached in an asymptotic sense). To take this fact into account, two different sets of data were taken for the optimisation process:

1. the interval of termination points
2. the mid-points of the relaxed stresses of the hysteresis

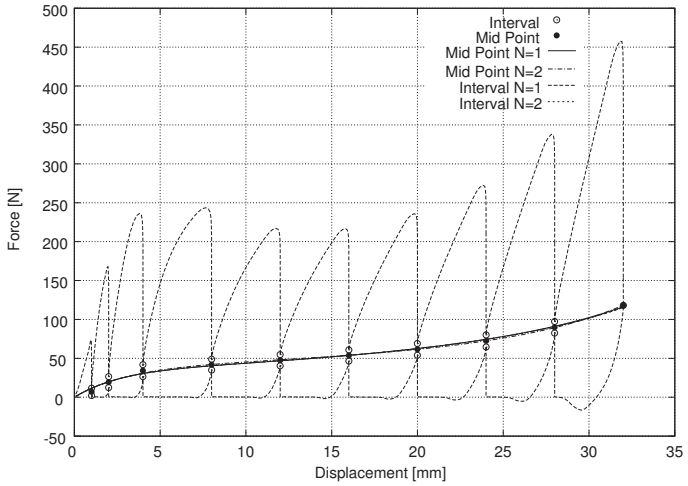

Figure 7: Optimisation results of the uniaxial compression test with different parameter sets (N = 1, N = 2), experimental data with holding times (dashed line), termination points of relaxation (open circles).

Parameter analysis. The first analysis concerns the parameter optimisation according to the force-stretch-relation (17) in the case N=1 and (14) and (15) in the case N=2 for the uniaxial compression test. The results are given in Table 1 and Figure 7.

Table 1: Parameter sets for the uniaxial compression test

	Mid-Point		**Interval**	
	***N*=1**	***N*=2**	***N*=1**	***N*=2**
Quality Function	3.63	3.62	6.76	6.76
$\mu_1 = \mu$ [MPa]	$0.857\ 10^{-2}$	$0.481\ 10^{-2}$	$0.831\ 10^{-2}$	$0.479\ 10^{-2}$
$\alpha_1 = \alpha$	$0.198\ 10^{2}$	$0.198\ 10^{2}$	$0.198\ 10^{2}$	$0.198\ 10^{2}$
$\beta_1 = \beta$	$0.105\ 10^{-1}$	$0.145\ 10^{-1}$	$0.109\ 10^{-1}$	$0.139\ 10^{-1}$
μ_2 [MPa]		$0.360\ 10^{-2}$		$0.351\ 10^{-2}$
α_2		$0.198\ 10^{2}$		$0.197\ 10^{2}$
β_2		$0.650\ 10^{-2}$		$0.657\ 10^{-2}$

It can be seen from Table 1 that the quality function for the used data set show almost no difference in the case $N = 1$ and $N = 2$. Furthermore the differences of the values of the parameters for the different cases (Mid-Points and Interval) are also negligible. This is also documented by almost congruent curvatures in Figure 7.

Table 2: Optimised parameter sets for the uniaxial compression test by the analytical solution (Numerical Fit) and FE-solver (FE Fit)

	Numerical Fit	**FE Fit**
μ [MPa]	$0.831\ 10^{-2}$	$0.907\ 10^{-2}$
α	$0.198\ 10^{2}$	$0.213\ 10^{2}$
β	$0.109\ 10^{-1}$	$0.849\ 10^{-2}$

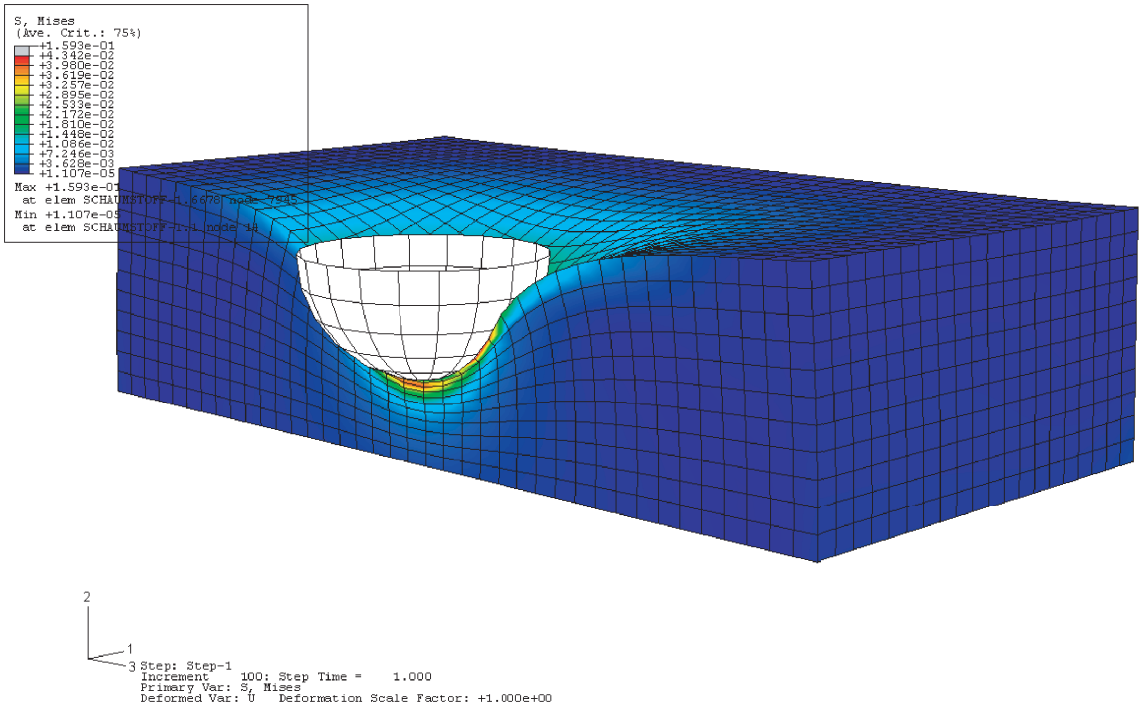

Figure 8: FE-simulation of the indenter test in a deformed state. The grey-scale indicates the reaction force between the indenter and the foam

FE-Simulation. Table 2 shows a comparison of the parameter determination for the uniaxial compression test derived from eq. (17) and an FE-simulation of this test. Figure 9 gives the results of this comparison between the experimental data of the indenter test (termination points) and the FE-simulation based on the constitutive equation (5) by using the parameter sets from the "FE Fit" of Table 2. The graph for the simulation apparently lies within the termination points of the indenter tests. Figure 8 shows the FE-simulation of the indenter test in a deformed state.

7 Conclusion and Discussion

The objective of this study was to investigate the appropriateness of a strain energy function for finite hyperelasticity proposed by Hill (1978), Storakers (1986) and Ogden (1972) to describe the elastic properties of soft foams. This strain energy function is implemented in the FE-program ABAQUS for highly compressible foams in a very similar form. To accomplish this goal the following three important steps were carried out:

1. Carrying out appropriate experiments
2. Performing a parameter identification of the constitutive equation
3. Performing a complex test loading experiment, simulating this experiment with a FE-tool by using the optimised parameter set and comparing the results with the experimental data

a.

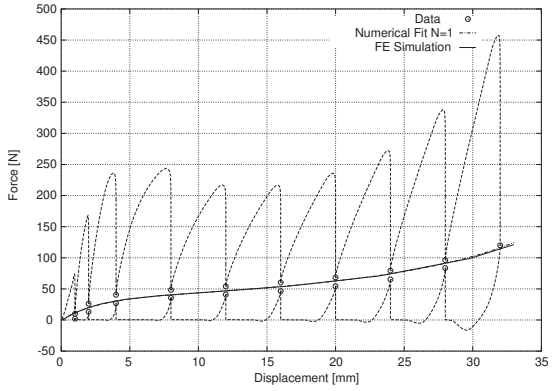

b.

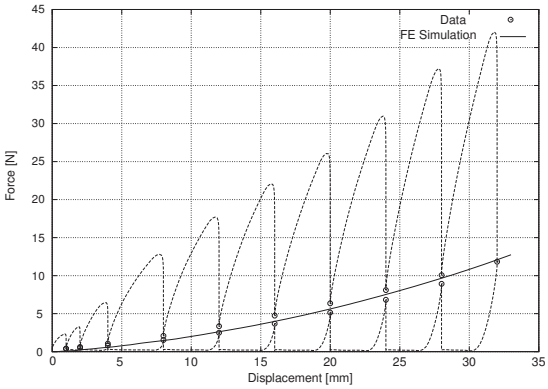

Figure 9: a. Comparison of the optimisation processes (Numerical Fit and FE Fit) by the uniaxial compression test (termination points), b. comparison of the experimental data of the indenter test and the FE-Simulation with a parameter set derived from the uniaxial compression tests.

The differing geometrical dimensions of the used test specimen from the standard cubes guarantee that the empirical tests are not influenced by the boundary conditions of the test specimens (buckling). The purpose of this study was to characterise the elastic properties of soft foams so that the elastic properties had to be separated from the inelastic ones by appropriate experiments. This was obtained by a cyclic preprocess to eliminate the MULLINS effect and approximate experiments after a recovery phase of 16 hours with a stepwise loading and unloading of the test specimen. At each load step a holding time of 180 min was kept. But even at this time period of constant deformation the overstress is not completely relieved. This is indicated by the gap of the lower and upper termination point of each loading step. Thus there is a range of uncertainty for the course of the elastic force displacement relation of the foam. This uncertainty was investigated by doing the parameter optimisation using the termination points for each step and the arithmetic mean of the holding points as well. The results of the two identification procedures are almost equal regarding the numerical values of the parameters (see Table 1). Table 1 also shows that there is almost no difference in the figures of the quality function for the different formulation of the strain energy function used here for $N = 1$ and $N = 2$. Thus for the examined materials there is no difference in using the mid-points or the lower and upper termination points for the parameter identification or setting $N = 1$ or $N = 2$ in the strain energy function.

In spite of the inhomogeneity of the deformation field in the uniaxial compression test caused by the boundary conditions (see Section 2) the FE-simulation does not provide a different result for the fit compared to the numerical one (see Figure 7 and Table 2). This probably indicates that the inhomogeneity of the deformation field is not a significant one.

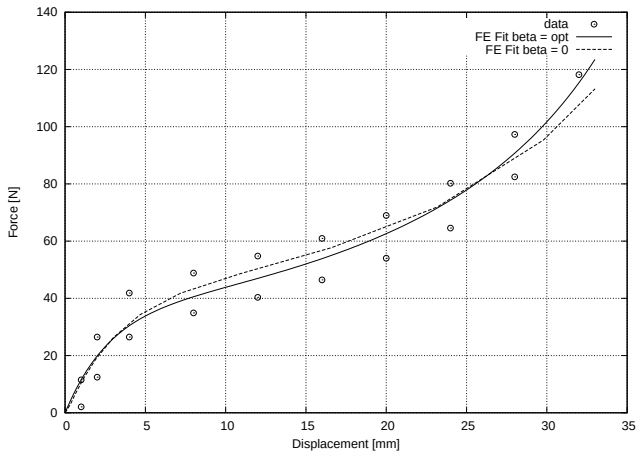

Figure 10: Comparison between the parameter optimisation for the constitutive equation (17) for $\beta = 0$ (dashed line) and $\beta \neq 0$ (solid line) being optimised using data from the uniaxial compression test.

The parameter β is not negligible as done by Mills and Gilchrist (2000). All parameter optimisations, regardless of whether the quality function was calculated using (17) or the FE-tool, β was significantly different from zero.

Beside this fact, if an optimisation is done for a parameter set with $\beta = 0$ the results as shown in Figure 10 indicate that such a parameter set underestimates the reaction force of the foam at large deformations. For the foams examined in this study this effect is tolerable. Whether this is also tolerable for different foams is arguable.

The appropriateness of the used strain energy function for describing the elastic properties of the examined soft foams is given if a complex loading scenario can be simulated with the parameter set derived from a simple load scenario. This complex scenario was generated by an indenter type test (see Figure 8). The result of the comparisons is given in Figure 9. The FE-simulation results lie in the corridor generated by the lower and upper termination points of the indenter test.

Acknowledgement

Preparatory work for this examination was made in the course of a project ,,Dekubitusprä-vention mit optimierten Schaumstoffprodukten (DekOS)“ funded by the ,,Bundesministerium für Forschung und Technologie“ of the Federal Republic of Germany. The authors want to thank Foam Partner Fritz Nauer AG (Wolfhausen, Switzerland) and Thomashilfen Technik + Innovation (Bremervörde, FRG) for providing the project with test specimens and financial support. Furthermore we want to thank Dr. Rainer Sievert (Bundesanstalt für Materialforschung und -prüfung, Berlin, FRG) for numerous seminal discussions and stimulations concerning this project.

References

Chagnon, G.; Marckmann, G.; Verron, E.; Gornet, L.; Charrier, P.; Ostoja-Kuczynski, E.: A new modelling of the mullins effect and the viscoelasticity of elastomer based on a physical approach. In: *Proceedings of the International Rubber Conference*. Prague, Czech Republic, (2002).

Czysz, H.-J.: *Experimentelle Untersuchungen an Polyurethan-Integralweichschaum zur Bestimmung von Kennwerten zu Berechnungsgrundlagen*. Ph.D. thesis, Universität der Bundeswehr Hamburg, (1986).

Ehlers, W.; Markert, B.: Viscoelastic polyurethane foams at finite deformations. In: Wall W. A., Bletzinger K. U. and Schweizerhof K. (Eds.), *Trends in Computational Structural Mechanics. CIMNE, Barcelona*, (2001), pp. 249–256.

Eipper, G.: *Theorie und Numerik finiter elastischer Deformationen in fluidgesättigten porösen Festkörpern*. In: Bericht Nr. II-1 aus dem Institut für Mechanik, Lehrstuhl II. Universität Stuttgart, (1998).

Green, A. E.; Adkins, J. E: *Large Elastic Deformations*, 2nd Edition. Oxford University Press, Oxford, (1970).

Hartmann, S.; Haupt, P.; Tschöpe, T.: Parameter identification with a direct search method using finite elements. In: *Constitutive Models for Rubber II. Balkema Publ., Lisse*, (2001), pp. 249–256.

Hartmann, S.; Tschöpe, T.; Schreiber, L.; Haupt, P.: Finite deformations of a carbonblack-filled rubber. experiment, optical measurement and material parameter identification using finite elements. *European Journal of Mechanics A/Solids*, 22, (2003), 309–324.

Hibbitt; Karlsson; Sorensen: *ABAQUS, Theory Manual, 6th Edition*. Abacom Software GmbH, (2000a).

Hibbitt; Karlsson; Sorensen: *ABAQUS, User‘s Manual, 6th Edition*. Abacom Software GmbH, (2000b).

Hill, R.: Aspects of invariance in solid mechanics. *Advances in Applied Mechanics*, 18, (1978), 1–75.

James, A. G.; Green, A.: Strain energy functions of rubber. ii the characterization of filled vilcanisates. *J. Appl. Plym. Sci.*, 19, (1975), 2033–2058.

Lenz, T.: Modellierung von Polymerschäumen. In: *Tagungshandbuch zur Fachtagung Polymerschäume – Perspektiven und Trends*, Würzburg, (1999).

Lion, A.: A constitutive model for carbon black filled rubber: Experimental investigations and mathematical representation. Continuum. *Mech. Thermodyn.*, 8, (1996), 153–169.

Mills, N. J.; Gilchrist, A.: Modelling the indentation of low density polymers foams. *Cellular Polymers*, 19, (2000), 389–412.

Mullins, L.: Softening of rubber by deformation. *Rubb. Chem. Technol.*, 42, (1969), 339–362.

Nelder, J. A.; Mead, R.: A simplex method for function minimization. *Comp. J.*, 7, (1969), 308–313.

Ogden, R. W.: Large deformations isotropic elasticity –on the correlation of theory and experiment for incompressible rubberlike solids. In: *Proceedings of the Royal Society of London, Series A*. Vol. 326., (1972), pp. 565–584.

Otten, R. H. J. M.; van Ginneken, L. P. P. P.: *The Annealing Algorithm*. Kluwer, Boston, (1989).

Reese, S.: *Theorie und Numerik des Stabilitätsverhaltens hyperelastischer Festkörper*. Ph.D. thesis, TH Darmstadt, (1994).

Renz, R.: *Zum zügigen und zyklischen Verformungsverhalten polymerer Hartschaumstoffe*. Ph.D. thesis, TH Karlsruhe, (1977).

Renz, R.: Modellvorstellungen zur Berechnung des mechanischen Verhaltens von Hartschaumstoffen. In: *Schaumkunststoffe*. Fachverband Schaumkunststoffe e.V, Düsseldorf, (1978).

Schwefel, H. P.: *Evolution and Optimum Seeking*. Wiley & Sons, New York, (1995).

Simo, J. C.; Taylor, R. L.: Quasi-incompressible finite elasticity in principal stretches. Continuum basis and numerical algorithms. *Computer Methods in Applied Mechanics and Engineering*, 85, (1991), 273–310.

Storakers, B.: On material representation and constitutive branching in finite compressible elasticity. *J. Mech. Phy. Solids*, 34 No 2, (1986), 125–145.

Van den Bogert, P. A. J.; de Borst, R.: On the behaviour of rubberlike materials in compression and shear. *Arch. Appl. Mech.*, 64, (1994), 136–146.

Wang, Y.; Cuitino, A. M.: Three-dimensional nonlinear open-cell foams with large deformations. *Journal of the Mechanics and Physics of Solids*, 48, (2000), 961–988.

Addresses:

M. Schrodt, G. Benderoth, G. Silber: FH Frankfurt, University of Applied Sciences, Institute for Material Science, Nibelungenplatz 1, D-60318 Frankfurt/Main

email:`schrodt@fb2.fh-frankfurt.de`

A. Kühhorn: Brandenburgische Technische Universität Cottbus, Engineering Mechanics and Vehicle Dynamics, Siemens-Halske-Ring 14, D-03046 Cottbus